



# An investigation of thermal aging effects on the mechanical properties of a Ni<sub>3</sub>Al-based alloy by nanoindentation

Dongyun Lee\*

Department of Nanomaterials Engineering & BK21 Nanofusion Technology Team, College of Nanoscience and Nanotechnology, Pusan National University, 30 Jangjeon-dong, Geumjeong-gu, Busan, 609-735, Republic of Korea

## ARTICLE INFO

### Article history:

Received 24 January 2009  
Received in revised form 4 February 2009  
Accepted 4 February 2009  
Available online 20 February 2009

### Keywords:

Intermetallics  
Grain boundaries  
Mechanical properties  
Microstructure  
Transmission electron microscopy

## ABSTRACT

Ni<sub>3</sub>Al-based intermetallic alloys are composed of a  $\gamma$  network and  $\gamma'$  domains. In general, through precipitation, the  $\gamma'$  phase is used as a hardening source for this alloy. This study examined how  $\gamma'$  acts as a hardening material in a cast Ni<sub>3</sub>Al-based intermetallic alloy. Specimens cut from a centrifugally cast tube were aged in Ar at elevated temperatures for up to 1600 h. Hardness tests were then performed in air at room temperature. Vickers microhardness and nanoindentation tests were carried out on specimens aged at 900 °C and 1100 °C. The microstructures were examined by scanning electron microscopy (SEM) and transmission electron microscopy (TEM). The microhardness of bulk Ni<sub>3</sub>Al decreased dramatically with increasing thermal aging time at 900 °C, but the nanohardness measured by the nanoindenter did not significantly decrease. The nanohardness data suggested that the hardening effects were caused by the precipitation of the  $\gamma'$  phase on the  $\gamma$  and  $\gamma'$  cells.

© 2009 Elsevier B.V. All rights reserved.

## 1. Introduction

For many years, L1<sub>2</sub>-type intermetallic alloys such as Ni<sub>3</sub>Al have struggled to attract the interest of scientists and engineers due to their brittle behavior at ambient temperatures even though these alloys have scientific and technological importance in structural applications. Recently, this drawback was overcome by alloying with elements such as boron [1–3] and zirconium [4]. The mechanical properties of Ni<sub>3</sub>Al could be improved significantly by modifying the microstructure using the appropriate alloying and processing techniques [5]. Ni<sub>3</sub>Al-based intermetallic alloys have recently been developed for industry applications, e.g., transfer rolls, high temperature bolts and nuts, and carburizing molds. In particular, a Ni–Al<sub>16.34</sub>–Cr<sub>7.86</sub>–Mo<sub>0.85</sub>–Zr<sub>1.23</sub>–B<sub>0.025</sub> at.% alloy known as ASTM A1002-99 (or IC221M) is currently being evaluated for important industrial applications [6–8]. IC221M basically consists of a small amount of a face-centered cubic  $\gamma$  network, the Ni solid solution phase, and a dominant  $\gamma'$ , the L1<sub>2</sub> ordered phase. The thermal aging effects on the microstructure and mechanical properties of Ni<sub>3</sub>Al-based intermetallic alloys have been studied extensively over the last few decades because of the high temperatures used for these alloys [5,6,9–11]. However, few studies have reported on how the individual domains ( $\gamma$  and  $\gamma'$  cells) are affected by thermal aging, particularly in terms of the mechanical properties. This letter

describes how the individual domains of the alloys are affected by thermal aging.

## 2. Experiments

To determine the intrinsic properties affected by thermal aging, specimens were first cut from a centrifugally cast tube and encapsulated in quartz tubes with Ar in preparation for the aging process. The specimens were then aged at 900 °C and 1100 °C for up to 1600 h. The as-cast and aged specimens were polished and etched with glyceric acid (30 ml glycerin, 30 ml HCl, and 15 ml HNO<sub>3</sub>) for metallographic examination. A nanoindentation system (Nanoindenter II™ and XP™; Agilent Technologies Inc., Oak Ridge, TN, USA) was used to determine how the single  $\gamma$  or  $\gamma'$  domains were affected by thermal aging. The results are presented as the average of 20 indents. The tests were carried out over a broad range of loads from 4 mN to 50 mN. The nanoindenter [12] is an instrument that can sense the depth during an indentation. It can be used to probe the mechanical properties of individual domains in an alloy; these domains are probably on the micron and/or submicron scale. The continuous stiffness module (CSM) technique was used in this study [12]. For comparison, the Vickers hardness results were used from a previous work [11]. All hardness values are expressed as pressures. The microstructures affected by thermal aging in Ar were observed by scanning electron microscopy (SEM) and transmission electron microscopy (TEM).

## 3. Results and discussion

Fig. 1 shows typical load–displacement curves (average of 20 indents) from nanoindentations in two distinctly different regions: the dendrite arms and the interdendritic regions. The primary difference between these regions is the relative volume fraction of  $\gamma'$ , which is higher in the vicinity of the interdendritic region [5,10,11,13]. The indentation depth was shallower in the interden-

\* Tel.: +82 55 350 5301; fax: +82 55 350 5653.  
E-mail address: [dlee@pusan.ac.kr](mailto:dlee@pusan.ac.kr).

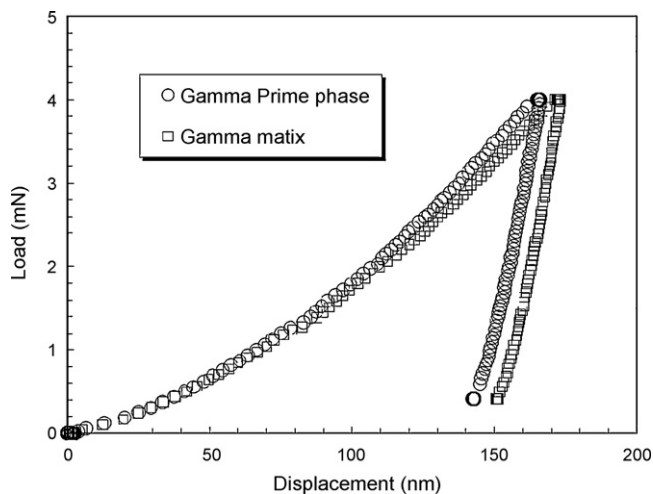


**Fig. 1.** Representative load-displacement curves of the  $\gamma$  and  $\gamma'$  phases of the as-cast material showing that the  $\gamma'$  phase is stronger than the  $\gamma$  phase.

driftic region due to the strengthening effect from the  $\gamma'$  phase [13,14]. The averaged hardness value of the interdendritic region was approximately 10% higher than that of the dendritic region (data not shown). Schöberl et al. [13] reported that the hardness of a  $\gamma'$  precipitate was much higher than that of the  $\gamma$  matrix. The  $\gamma'$  phase is often used as a strengthening source through a precipitation process or mixing with the soft matrix [15]. As such, the  $\gamma'$  precipitates in IC221M also acted as a strengthening source. Moreover, pop-in events were observed at a load of approximately 1.4 mN, which has also been reported elsewhere [16].

Fig. 2 shows the difference in the microstructure before and after aging at 900 °C. The SEM micrographs in Fig. 2a and b show the microstructures of the dendrite core for the as-cast and 1600 h aged specimens, respectively. The  $\gamma$  and  $\gamma'$  cells clearly coarsened with aging time at 900 °C. The TEM micrographs in Fig. 2c and d confirmed that the  $\gamma$  and  $\gamma'$  phases coarsened with increasing aging time and suggested that coalescence was responsible for this behavior. The arrows “a” indicate that some of the coarse domains appeared to have formed through the coalescence of several previously existing domains. Presumably, coarsening of the  $\gamma$  and  $\gamma'$  phases with increasing aging time at elevated temperatures was another factor that reduced the room temperature tensile strength and microhardness [17], as reported in a previous study [11].

The results of the nanoindentation examinations are shown in Fig. 3a. The nanoindentation hardness was measured at a load of 20 mN. The modulus of IC221M was approximately 210 GPa, which was in good agreement with the literature value [18]. The hardness of the as-cast alloy was approximately 4.5 GPa, which was significantly higher than the Vickers hardness. This was largely due to the indentation size effect [19]. This was also observed in the hardness measurements from both the Vickers indenter and the nanoindenter. The hardness obtained from a nanoindentation load of 4 mN was  $\sim$ 5.5 GPa, as shown in Fig. 1. Fig. 3b shows the change in hardness according to the Vickers tests. The load decreased with increasing Vickers hardness and approached the load in the nanoindentation tests. It is assumed that the surface effects on the nanohardness might be minimized since the specimens were chemically etched and indentation depth were about half micron.

The Vickers microhardness (load 300 gf) of the alloy aged in Ar at 900 °C and 1100 °C as a function of the aging time has been reported elsewhere [5,11]. The microhardness of the specimen aged at 900 °C decreased dramatically (>15%) after aging for 72 h. The

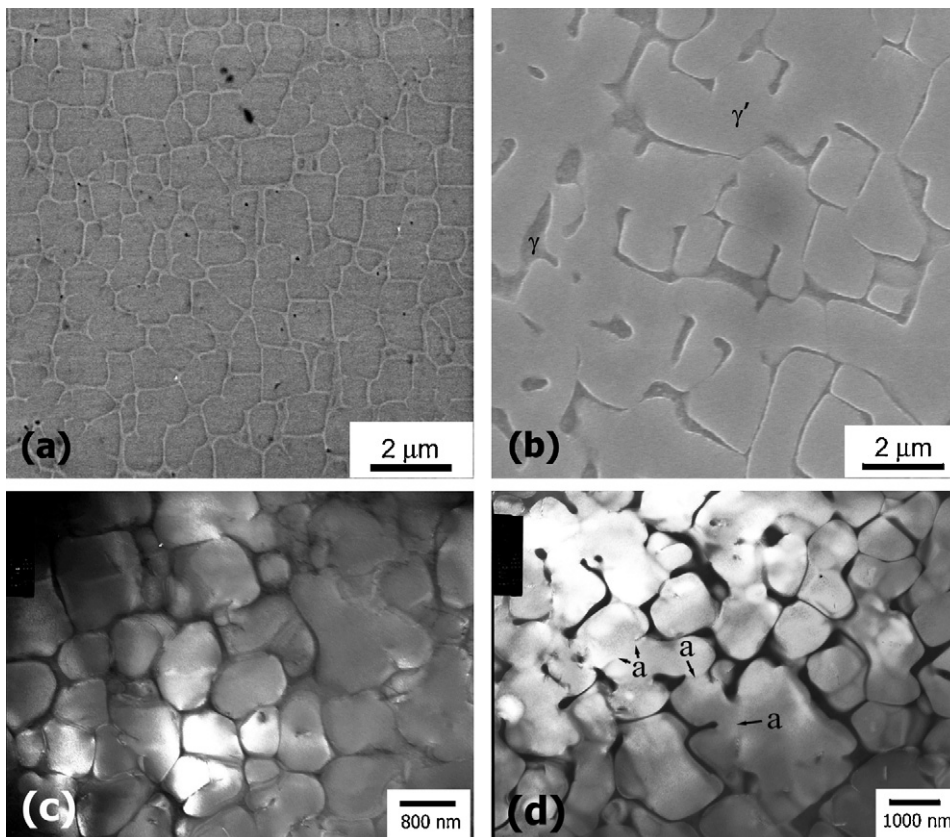


**Fig. 2.** Micrographs of as-cast and aged IC221M at 900 °C as a function of the aging time: SEM micrographs of (a) as-cast and (b) 1600 h specimens; TEM micrographs of (c) as-cast and (d) 100 h specimens.

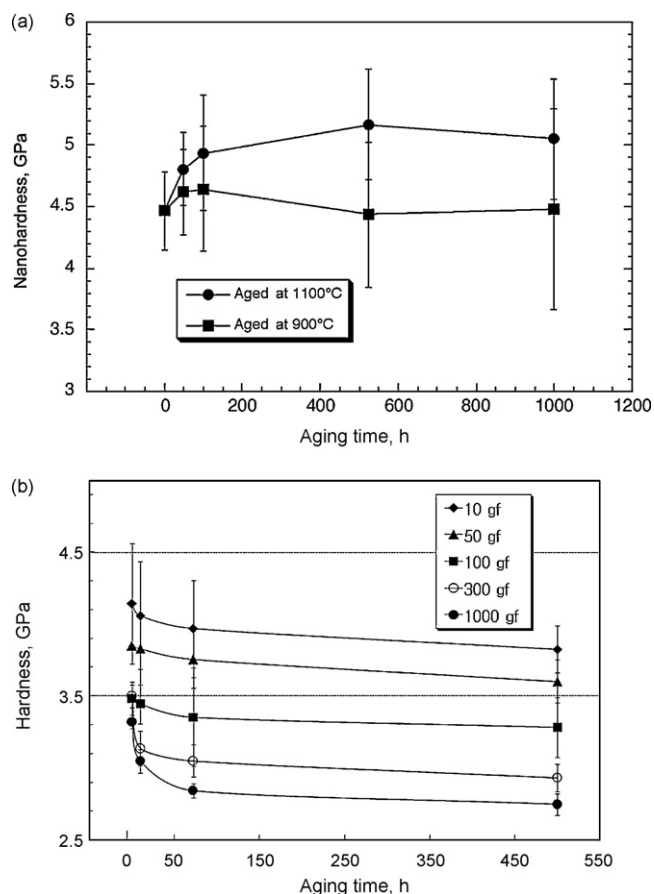


**Fig. 3.** Variation in the IC221M hardness as a function of the aging time: (a) change in nanoindentation hardness tested at 20 mN as a function of the aging time at 900 °C and 1100 °C, (b) variation in Vickers microhardness for a specimen aged at 900 °C as a function of the aging time for various indentation loads.

sharp decrease in hardness after a short aging time was consistent with results from a tensile test in which a decrease in the yield strength was observed [11]. As previously noted, the mechanistic origins of the phenomena presumably resulted from a thermally activated rearrangement of the  $\gamma$  and  $\gamma'$  phases (e.g., change of volume fraction, coarsening), thermal energy-induced relaxation of the residual stress, and/or the redistribution of chemical species due to microsegregation [7,11,20]. The hardness of the specimen aged at 1100 °C decreased slightly when aged for a short time, but it increased to a stable value similar to the hardness of the original as-cast alloy.

Note that the sharp decrease in Vickers microhardness after short-term aging was reduced by decreasing the indentation load, as shown in Fig. 3b. Furthermore, the nanoindentation results showed that while the Vickers hardness decreased for a specimen subjected to short-term aging at 900 °C, the nanoindentation hardness did not; it increased with increasing aging time. The nanoindentation hardness of the specimen aged at 1100 °C also showed an increase with increasing annealing time. In contrast to the Vickers hardness, no decrease in hardness occurred even after short-term annealing (50 h). The area covered by the Vickers indent was clearly larger than that sampled by the nanoindentation indents. Furthermore, this result suggested that the interfaces between the  $\gamma$  and  $\gamma'$  domains were weak links. The schematic diagram shown in Fig. 4 indicates that the Vickers hardness impressions deformed several  $\gamma$  and  $\gamma'$  domains such that an effect of the domain size on the hardness would be expected. The nanoindenter, however, deformed only one domain, suggesting that the degrada-

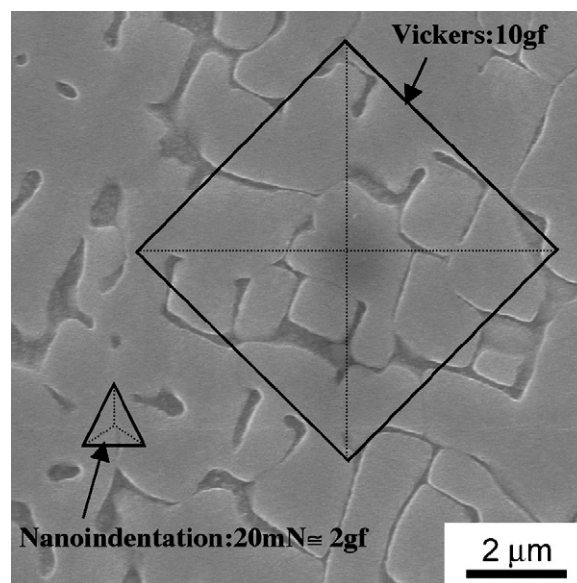


**Fig. 4.** A schematic diagram of the indent size relative to the microstructure of a specimen aged for 1600 h at 900 °C. The diamond represents the Vickers indent at a load of 10 gf, and the triangle indicates the nanoindentation at 20 mN  $\cong$  2 gf.

tion of the mechanical properties of the individual  $\gamma$  and  $\gamma'$  domains by thermal aging was not significant but improved slightly due to the reprecipitation of fine  $\gamma'$ . Therefore, the decrease in Vickers microhardness and tensile strength were mainly due to the domain boundaries. Previously, one of the main reasons for the increase in Vickers microhardness of specimens aged at 1100 °C was a volume fraction change in  $\gamma'$ . This may be one of the mechanistic origins for the increased hardness of  $\gamma$  or  $\gamma'$  cells for a specimen aged at 900 °C.

#### 4. Conclusions

The nanoindentation experiments provided insight into the extent to which the hardness and modulus depended on the compound's aging time and temperature; the aging process basically changed the compositions of the compound. These results suggested that the mechanical properties of the individual domains in the  $\gamma$  and  $\gamma'$  phases did not degrade with thermal aging but improved slightly due to the reprecipitation of fine  $\gamma'$ . More reliable intermetallic compounds with good high-temperature mechanical properties might be obtained if the number of the  $\gamma$  and  $\gamma'$  domain boundaries can be reduced.

#### Acknowledgment

This work was supported for 2 years by Pusan National University Research Grant. This research was also sponsored by the U.S. Department of Energy, Assistant Secretary for Energy Efficiency and Renewable Energy, Industrial Materials for the Future Program and the Division of Materials Sciences and Engineering under contract DE-AC05-00OR22725 with UT-Battelle, LLC. The author wishes to thank Prof. G.M. Pharr at UT and Dr. M.L. Santella at ORNL, TN, USA for support and valuable advice.

#### References

- [1] K. Aoki, O. Izumi, *Nippon Kinzoku Gakkaishi* 43 (1979) 1190–1195.
- [2] C.T. Liu, J.O. Stiegler, *Science* 226 (1984) 636–642.
- [3] C.T. Liu, V.K. Sikka, *JOM* 38 (1986) 19–21.
- [4] E.P. George, C.T. Liu, D.P. Pope, *Scripta Metall. Mater.* 28 (1993) 857–862.
- [5] M. Florian, *Kov. Mater.-Met. Mater.* 41 (2003) 73–83.

- [6] V.K. Sikka, S.C. Deevi, S. Viswanathan, R.W. Swindeman, M.L. Santella, *Intermetallics* 8 (2000) 1329–1337.
- [7] D. Lee, M.L. Santella, I.M. Anderson, G.M. Pharr, *Intermetallics* 13 (2005) 187–196.
- [8] V.K. Sikka, M.L. Santella, P. Angelini, J. Mengel, R. Petrusha, A.P. Martocci, R.I. Pankiw, *Intermetallics* 12 (2004) 837–844.
- [9] J. Lapin, S. Wierzbinski, T. Pelachova, *Intermetallics* 7 (1999) 705–715.
- [10] J. Lapin, T. Pelachova, O. Bajana, *Intermetallics* 8 (2000) 1417–1427.
- [11] D. Lee, M.L. Santella, *Mater. Sci. Eng. A* 428 (2006) 196–204.
- [12] W.C. Oliver, G.M. Pharr, *J. Mater. Res.* 7 (1992) 1564–1572.
- [13] T. Schöberl, H.S. Gupta, P. Fratzl, *Mater. Sci. Eng. A* 363 (2003) 211–220.
- [14] M. Goken, M. Kempf, *Acta Mater.* 47 (1999) 1043–1052.
- [15] K. Mizuuchi, K. Inoue, M. Sugioka, M. Itami, J.H. Lee, M. Kawahara, *Mater. Sci. Eng. A* 428 (2006) 169–174.
- [16] W. Wang, C.B. Jiang, K. Lu, *Acta Mater.* 52 (2003) 6169–6180.
- [17] S.Q. Zhao, X.S. Xie, G.D. Smith, S.J. Patel, *Mater. Lett.* 58 (2004) 1784–1787.
- [18] V.K. Sikka, in: S.C. Deevi (Ed.), *International Symposium on Nickel and Iron Aluminides*, ASM International, 1997, pp. 361–378.
- [19] J.G. Swadener, E.P. George, G.M. Pharr, *J. Mech. Phys. Solids* 50 (2002) 681–694.
- [20] D.P. Pope, S.S. Ezz, *Int. Met. Rev.* 29 (1984) 136–167.